Supporting Information

Bessaïh *et al.* 10.1073/pnas.0801484105

SI Text

Slice Preparation. A block of tissue containing the thalamus was removed and placed in a cold (<4°C) oxygenated (95% O_2 : 5% CO_2) solution of artificial cerebrospinal fluid: 125 mM NaCl, 2.5 mM KCl, 1 mM $CaCl_2$, 2 mM $MgCl_2$, 1.25 mM NaH_2PO_4, 26 mM $NaHCO_3$, 25 mM glucose, and 1 mM kynurenic acid (pH 7.3, osmolarity 310 mOsm). The block of tissue was glued, ventral surface uppermost, to the stage of a vibroslice (HV650V; Microm), and 300-μm thick horizontal sections containing the ventrobasal nucleus and the nucleus reticularis were prepared by using the internal capsule and the medial lemniscus as landmarks.

Slices (three to four per hemisphere) were stored in an oxygenated incubation chamber containing artificial cerebrospinal fluid of the above composition, but without kynurenic acid and with $MgCl_2$ 1 mM and $CaCl_2$ 2 mM for at least 1 h before being transferred to the recording chamber. There they were continuously perfused (1.5 ml/min) with warmed (32 ± 1°C) oxygenated recording solution. Experiments were performed on only a single neuron in a slice, after which the slice was discarded.

Model. ***T current.*** The model uses the Goldman-Hodgkin-Katz formulation for I_T as:

$$I_T = P\mathrm{max}_T.O.\frac{Vz^2F^2}{RT_k}\left[\frac{\mathrm{Ca}_{\mathrm{int}} - \mathrm{Ca}_{\mathrm{ext}}\exp\left(-\frac{VzF}{RT_k}\right)}{1-\exp\left(-\frac{VzF}{RT_k}\right)}\right]$$

where Pmax_T is the maximum permeability. $z = 2$ is the valence; $T_k = 298$K is the absolute temperature; F is the Faraday's constant; R is the gas constant, $\mathrm{Ca}_{\mathrm{int}} = 50$ nM and $\mathrm{Ca}_{\mathrm{ext}} = 2$ mM are the intracellular and extracellular Ca^{2+} concentrations, respectively; and O is the fraction of the T channel population in the open state.

The kinetic schemes for gating of T channels (1) comprised three closed states and one open state, each of them interconnected with an inactivated state, and therefore is composed of three loops (see Scheme S1). The transitions between closed states and between inactivated states are voltage-dependent, but transitions between closed and inactivated states are voltage-independent, as is the open-to-inactivated state transition. Rate constants for the transition C_3 to 0 (C_3 to I_3) were equalized to the ones for transition I_3 to I_4 (O to I_4 respectively).

The voltage-dependant rate constants were described by the following equations:

In the activation (forward) direction:

$$kx_n(V) = kx_n\exp\left(\frac{d_n q_n V}{T}\right).$$

In the deactivation (backward) direction:

$$kx_{-n}(V) = kx_{-n}\exp\left(\frac{(1-d_n)q_n V}{T}\right),$$

where x = c for transition between closed states or i for transition between inactivated states, and n = 1, 2 or 3 indicates the corresponding loop in the kinetic scheme (numbered from left to right).

$T = 25.6$ mV represents the thermal energy associated with the simulation temperature; q_n represents the gating charge associated with the nth loop in the model; the parameter d_n represents the fraction of the voltage dependence associated with kinetics of the transition in the forward direction. Parameter values used to model voltage-dependent and -independent transitions are summarized in Tables 1 and 2, respectively.

Transient K^+ current of type A. The transient K^+ current of type A (I_A) was generated by a Hodgkin–Huxley-like model, introduced by Huguenard and McCormick (2) and Gutierrez *et al.* (3):

$$I_A = g_A m^4 h(V - V_k)$$

with $V_k = -105$ mV;

$$m_\infty = \frac{1}{1+\exp\left(-\frac{V+60}{8.5}\right)};$$

$$\tau_m = \frac{1}{\exp\left(\frac{V+35.82}{19.69}\right)+\exp\left(-\frac{V+79.69}{12.7}\right)} + 0.37$$

$$h_\infty = \frac{1}{1+\exp\left(\frac{V+78}{6}\right)};$$

$$\tau_h = \frac{1}{exp\left(\frac{V+46.05}{5}\right)+\exp\left(-\frac{V+238.4}{37.45}\right)}$$

if $V < -63$ mV; and

$$\tau_h = 19; \text{ if } V \geq -63 \text{ mV}$$

h current. The h current was simulated by a Hodgkin–Huxley-like model, introduced by Huguenard and McCormick (2):

$$I_h = g_h m(V - V_h)$$

with $V_h = -43$ mV;

$$m_\infty = \frac{1}{1+\exp\left(\frac{V+75}{5.5}\right)};$$

$$\tau_m = \frac{1}{\exp(-14.59 - 0.086 \times V) + \exp(-1.87 + 0.0701 \times V)}.$$

Leak current. The leakage current was modeled by the sum of a Na^+ and K^+ current as follows:

$$I_{\mathrm{leak}} = g_{\mathrm{Na}}(V - V_{\mathrm{Na}}) + g_{\mathrm{KT}}(V - V_k)$$

with $V_{\mathrm{Na}} = 50$ mV.

Dynamic Clamp. The Ih conductance was simulated by a Hodgkin–Huxley-like model (see *Model*), using a real time version of the Neuron environment (developed by G. Le Masson; ref. 4) running under the Windows XP operating system. A PCI DSP

Board (Innovative Integration) was used to achieve data transfer between the computer and the patch-clamp amplifier to inject the simulated h current and monitor the membrane potential in real time.

1. Lambert RC, Bessaïh T, Leresche N (2005) Biophysical mechanisms underlying the paradoxical potentiation of the low-voltage activated calcium current in thalamocortical neurons: A modeling study. *Thalamus Relat Syst* 3:165–173.
2. Huguenard JR, McCormick DA (1992) Simulation of the currents involved in rhythmic oscillations in thalamic relay neurons. *J Neurophysiol* 68:1373–1383.
3. Gutierrez C, Cox CL, Rinzel J, Sherman SM (2001) Dynamics of low-threshold spike activation in relay neurons of the cat lateral geniculate nucleus. *J Neurosci* 21:1022–1032.
4. Wolfart J, Debay D, Le Masson G, Destexhe A, Bal T (2005) Synaptic background activity controls spike transfer from thalamus to cortex. *Nat Neurosci* 8:1760–1767.

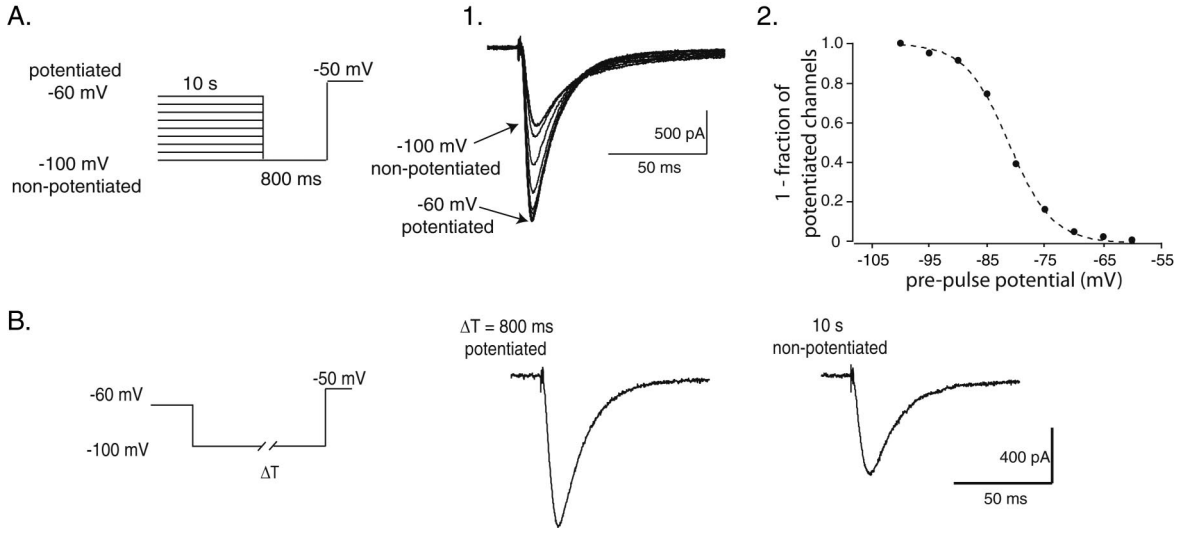

Fig. S1. Basic properties of IT potentiation. (*A*) To control the potentiated state of the channel population, TC neurons were conditioned by 10-s prepulses at various potentials (range: −60 to −100 mV). IT were thereafter evoked at −50 mV after an 800-ms hyperpolarization to −100 mV to allow recovery from inactivation. (*1*) Superimposed currents obtained with different prepulse potentials illustrate the increase in current amplitude with the increasing prepulse potential. 2. For each conditioning prepulse, the amplitude of the current was divided by the amplitude of the current obtained with the −60 mV prepulse. The graph presenting the fraction of the channels population in a nonpotentiated state (1-fraction of potentiated channels) that was estimated by normalizing the amplitude ratio, shows that the T current potentiation displays voltage dependence similar to that in the steady-state inactivation of the channel. (*B*) Currents were evoked at −50 mV after transient hyperpolarization of 0.8- and 10-s duration, respectively. Hyperpolarizations of 0.8-s are long enough to induce a full recovery from inactivation with only a partial depotentiation of the T channel population. In contrast, during the 10-s hyperpolarization to −100 mV, the full recovery from inactivation is associated with a nearly complete depotentiation resulting in a current of smaller amplitude. To record Ca^{2+} currents, electrodes were filled with 110 mM CsCl, 1 mM $CaCl_2$, 5 mM $MgCl_2$, 10 mM Bapta, 10 mM Hepes, 4 mM Na-ATP, and 15 mM phosphocreatine and 50 units/ml creatine phosphokinase (pH 7.3) 305 mOsm. Values of access resistance: 4–6 MΩ. At least 70% of the cell capacitance and series resistances were compensated. Leak currents were subtracted off line. To isolate the currents the following were added to the extracellular solution: 10 mM TEA, 1 mM 4-AP, 0.5 μM TTX, 2 mM CsCl, and 1 μM SR95531 (Tocris).

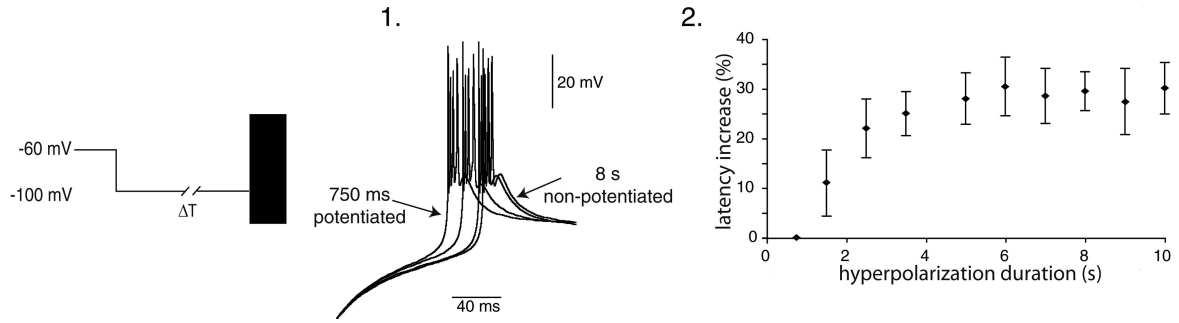

Fig. S2. Effect of the hyperpolarization duration on the LTS kinetics. Transient hyperpolarizations to −100 mV of increasing durations (range: 0.75–10 s) were performed in voltage-clamp mode to progressively decrease the number of T channels in the potentiated states. Every hyperpolarization is long enough to induce the full recovery from inactivation of the whole T channel population. The LTSs were thereafter recorded upon membrane repolarization in the current-clamp mode. 1. The superimposed traces that present typical LTSs evoked in a cell successively submitted to 0.75-, 1.5-, 3.5-, and 8-s hyperpolarizing prepulses, show the increase in the onset of the LTS resulting from the lengthening of the conditioning prepulse that reduces the amount of T channels in the potentiated state. 2. In 6 cells submitted to the same protocol, the time laps between the repolarization onset and the first action potential was measured and normalized to the value obtained for LTSs evoked after the minimal hyperpolarization duration (0.75 s). The graph presents the mean normalized values as a function of the hyperpolarization duration.

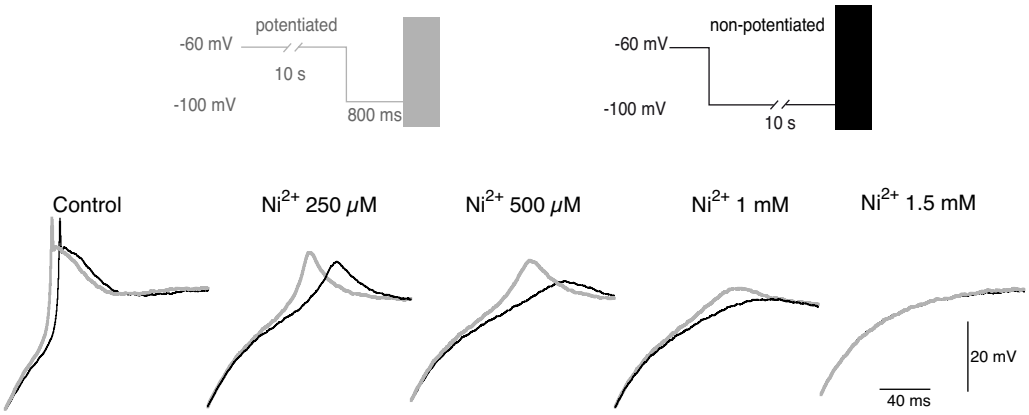

Fig. S3. Effects of increasing doses of nickel. LTSs were evoked in the presence of TTX on the offset of hyperpolarization to −100 mV of either 0.8 (gray traces) or 10-s duration (black traces). In control conditions, IT potentiation only affects the onset kinetics of the LTS without modifying its amplitude. In the same TC neuron successively submitted to increasing concentrations of Ni^{2+} (from 250 μM to 1.5 mM), the channel potentiation clearly affects the LTS amplitude and dramatically modulates the LTS kinetics when intermediate concentrations of Ni^{2+} (250 μM to 1 mM) that block part of the T channel population were applied. When T channels are totally blocked (right traces), the neuron presented similar passive membrane repolarization with the two protocols.

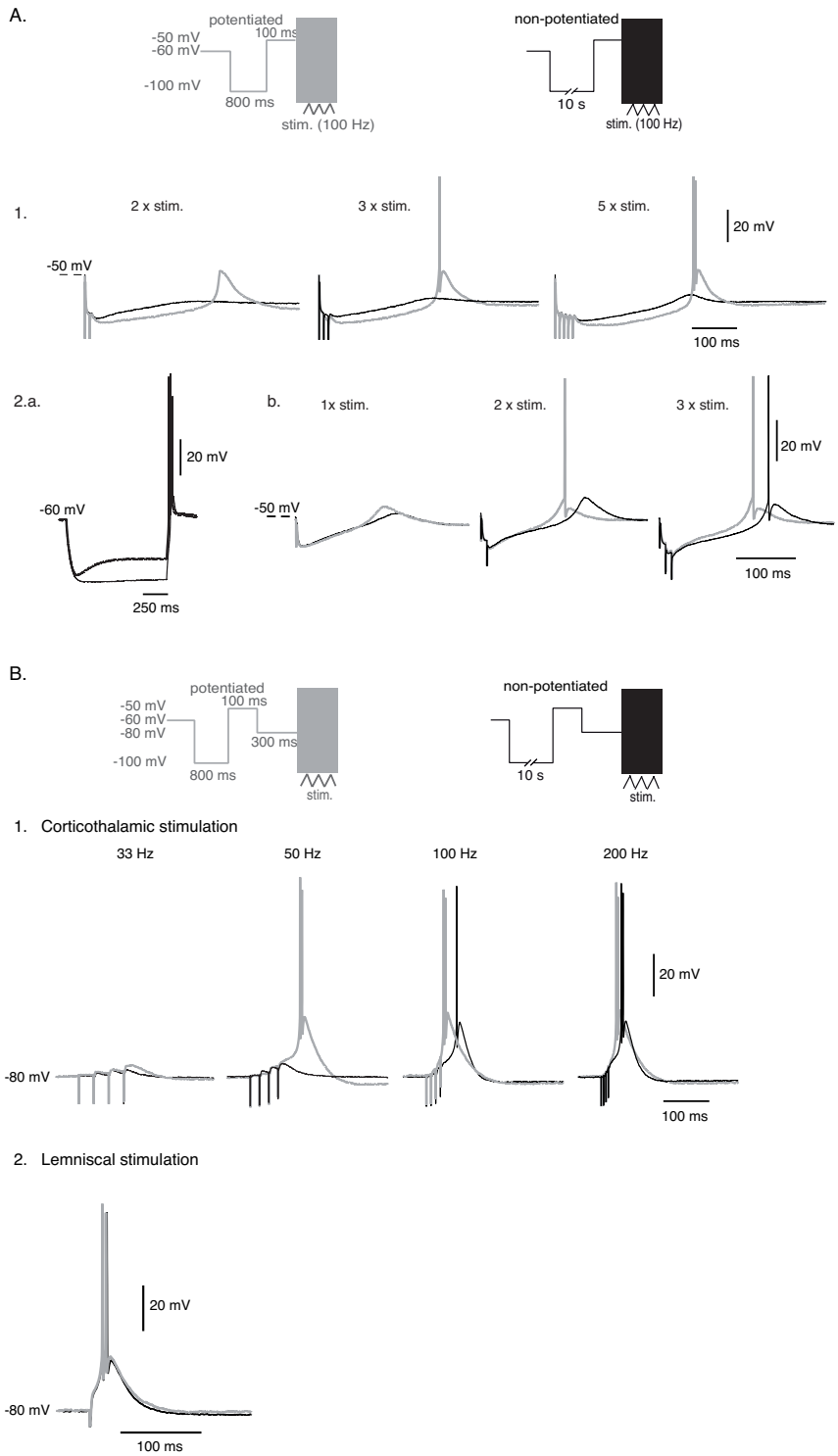

Fig. S4. Impact of IT potentiation on synaptic integrative properties in the presence of Ih. (*A*) Conditioning prepulses to −100 mV were used to set the whole T channel population either in a potentiated (800 ms; gray traces) or nonpotentiated state (10 s; black traces), as in Fig. 4*A*. Channels were thereafter inactivated at −50 mV for 100-ms and LTSs were evoked by local stimuli of the GABAergic NRT inputs. (*1*) Traces show typical rebound LTSs evoked in the absence of Ih blocker in a TC neuron successively submitted to 2, 3 and 5 local stimulations at 100 Hz. Similar results were observed in five cells. Note that full size rebound LTSs are only evoked after 800-ms conditioning prepulses that induce the T channel potentiation. Note also that, because of the difference in the amplitude of Ih evoked in both conditions, local stimulation of the NRT input induced weaker and shorter transient hyperpolarisation after 10-s than after 800-ms prepulses to −100 mV. (*2*) The experiments presented in *1* do not allow to distinguish whether the observed effects on the LTS generation are due to the T channel potentiation or to differences in Ih activation. Therefore, similar experiments were performed by using the dynamic-clamp method (see *SI Text*, *Dynamic Clamp* for details) to reintroduce an artificial h conductance in the presence of Ih blocker ($n = 6$). This approach allowed to add an h conductance specifically during local stimulation and rebound generation and therefore to avoid the artefactual Ih activation that occurred during the conditioning prepulses. (*2a*) In the presence of 50 μM ZD 7288, the membrane potential response to hyperpolarizing current injections (1 s, −200pA) did not display the typical sag (thin trace) due to Ih activation. However, this sag is reestablished when artificial h conductance is added by the dynamic-clamp method (thick trace). (*2b*) Traces show typical rebound LTSs evoked with potentiated (gray traces) and nonpotentiated (black traces) T channels in a TC neuron successively submitted to one, two, and three local stimulations at 100Hz in the presence of artificial Ih. Note that IT potentiation clearly facilitates LTSs generation and associated firing and accelerate its onset kinetics. Therefore, the progressive recruitment of Ih during PPSI summation does not counteract the effect of IT potentiation on the burst generation. (*B*) In the absence of Ih blocker, LTSs were evoked by stimulations of either the corticothalamic (*1*) or the lemniscal pathway (*2*), as in Fig. 4*B*. T channels were forced in the inactivated and potentiated states (gray traces) or inactivated and nonpotentiated states (black traces), using conditioning prepulses similar to those in *A*. Stimulations were thereafter performed after a 300-ms hyperpolarization to −80 mV to induce the recovery from inactivation of a large fraction of the T channel population. Due to the difference in Ih activation, the membrane potential reached when the amplifier was switched to the current clamp mode was different for the two conditioning protocols. This difference was therefore compensated by injecting a hyperpolarizing current to match the voltage levels before stimulating the excitatory afferents. 1. Note that the presence of Ih does not change the effects of the IT potentiation on the probability, latency and amplitude of LTSs generated by stimulation of the corticothalamic pathway (compare to Fig. 4*B*1). (*2*) Similarly, no effect of the IT potentiation on the amplitude or kinetics of the LTSs evoked by the sensory EPSPs induced by stimulation of the lemniscal pathway in the presence of Ih.

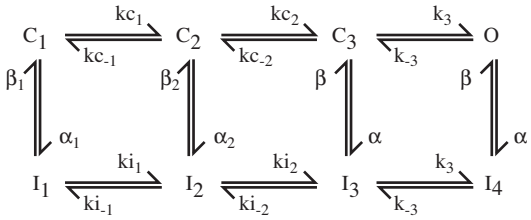

Scheme S1. Kinetic schemes for gating of T channels.

Table S1. Voltage-dependent rate constants (in ms^{-1})

Rate constant	ms^{-1}
kc_1	9
kc_2	13.05
k_3	0.16
kc_{-1}	0.162
kc_{-2}	7.47×10^{-3}
k_{-3}	3.15×10^{-3}
ki_1	0.86
ki_2	0.71
ki_{-1}	6×10^{-3}
ki_{-2}	4.3×10^{-7}
d_1	0.8
d_2	0.26
d_3	0
q_1	2.24
q_2	3.81
q_3	0.79

Table S2. Voltage-independent rate constants (in ms^{-1})

Current	Rate constant	ms^{-1}
Nonpotentiated	$\alpha 1$	8×10^{-4}
	$\alpha 2$	2.3×10^{-3}
	α	7.5×10^{-2}
	$\beta 1$	3×10^{-3}
	$\beta 2$	3.3×10^{-3}
	β	1.15×10^{-4}
Potentiated	α	8.45×10^{-2}
	β	1.3×10^{-4}

The values α and β were adjusted to mimic the acceleration in inactivation kinetics of the potentiated channels.